Mathematical framework for a place code in the auditory system

Alex D. Reyes[1]

[1]Center for Neural Science, New York University, New York, NY, USA

Abstract

A distinct feature of the auditory system is the tonotopic organization where the preferred frequency of neurons changes systematically along one axis. Tonotopy is postulated to be substrate for a place code, where sound frequency is encoded by the location of the neurons that fire during the stimulus. Though conceptually simple, the computations that allow for the representation of intensity and complex sounds is poorly understood. Here, the mathematical framework for place code is developed. The analyses suggest that the functional architecture, or topology, consists of overlapping neuron clusters whose size varies with intensity. Algebraic operations are derived to elucidate the rules for representing and assembling multi-frequency sound in networks and for modulating them with inhibition. Results obtained with network simulations are consistent with the general predictions. The analyses reveal the advantages and limitations of a place code and provide a mathematical foundation for building computational models and for interpreting experimental data.

Introduction

Many sensory systems are organized topographically so that adjacent neurons have small differences in the receptive fields. The result is that small changes in the sensory features causes an incremental shift in the spatial distribution of active neurons. This is has led to the notion of a place code where the location of the active neurons provides information about sensory attributes. In the auditory system, the substrate for a place code is tonotopy, where the preferred frequency of each neuron varies systematically along one axis [1]. Tonotopy originates in the cochlea [2, 3] and is inherited by progressively higher order structures along the auditory pathway [4]. The importance of a place code [5] is supported by the fact that cochlear implants, arguably the most successful brain-machine interface, enable deaf patients to discriminate tone pitch simply by delivering brief electrical pulses at points of the cochlea corresponding to specific frequencies [6].

Although frequency and intensity may be encoded in several ways [7], there are regimes where place-coding seems advantageous. Humans are able to discriminate small differences in frequencies and intensities even for stimuli as brief as 5-10 ms [8, 9, 10, 11]. Therefore, the major computations have already taken place within a few milliseconds. This is of some significance because in this short time interval, cortical neurons can fire only bursts of 1-2 action potentials [12, 13], suggesting that neurons essentially function as binary units. Therefore, it seems unlikely that neither frequency nor intensity can be encoded via the firing rate of cells since the dynamic range would be severely

limited. Similarly, coding schemes based on temporal or 'volley' schemes is difficult to implement at the level of cortex, because neurons can phase-lock only to low frequency sounds [14, 15, 16].

There are. however, several challenges with implementing a place coding scheme. First, the optimal architecture for representing frequency is not well-established. Possible functional units include individual neurons, cortical columns [17, 18], or overlapping clusters [19]. The dimension of each unit ultimately determines the range and resolution at which frequencies and intensities that can be represented and discriminated. Second, how both frequency and intensity can be encoded with a place code is unclear, particularly for brief stimuli when cells function mostly as binary units. Third, the rules for combining multiple stimuli is lacking. Physiological sounds are composed of pure tones with differing frequencies and intensities, resulting in potentially complex spatial activity patterns in networks. Finally, the role of inhibition in a place coding scheme is not well defined.

Here, a mathematical model is developed in order to gain insights into: 1) the functional organization of the auditory system that supports a place coding scheme for frequency and intensity: and 2) the computations that can be performed in networks. The approach is to use principles from set theory and topology to construct the acoustic and neural spaces, find a mapping between the spaces, and then develop the algebraic operations. The predictions of the math model are then examined with simulations.

Results

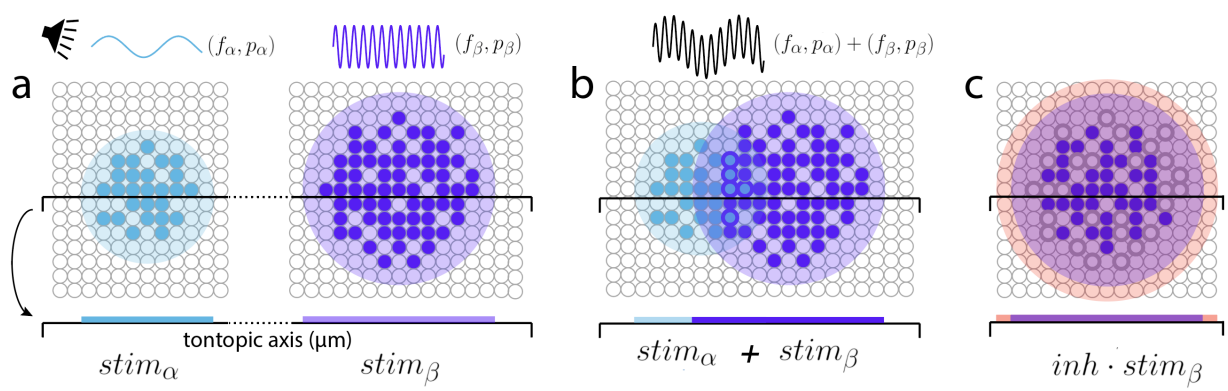

Figure 1: **Computations with a place code**. ***a, left***, hypothetical neural representation of a low frequency (f_α), small amplitude (p_α) pure tone stimulus in a two-dimensional neural network. A stimulus-evoked synaptic field covers a circular area (cyan disk) and causes a subset of cells to fire (filled circles). Projection of the synaptic field onto the tonotopic axis (bar) gives the location and size of the activated area. ***Right***, synaptic field generated by a tone of higher frequency (f_β) and sound pressure (p_β) pure tone. ***b***, synaptic field generated by a sound composed of the two tones. ***c***, modulation of the synaptic field and activated neurons by inhibition (red).

The mathematical model is subject on the following biological constraints. First, the neural space inherits the tonotopic organization of the cochlea [2, 3] so that the preferred frequency of neurons changes systematically with location along one axis. Second, a pure tone activates a population of neurons within a confined area [20], with the location of the area varying with the tone frequency. Third, the size of the activated area grows with sound intensity [20], paralleling

the increase in the spatial extent of the traveling wave in the cochlea [21, 22]. The model is broadly related to the "spread-of-excitation" class of models [7, 23]

The basic computations that can be performed using a place code are shown schematically in a 2-dimensional network of neurons (Fig. 1). In response to a pure tone stimulus, a synaptic field is generated within an enclosed area of the network (a, *left* cyan disk), causing a population of cells to fire (filled smaller disks). A tone with a higher frequency and intensity activates a larger area at a different location (*right*). A sound composed of the two pure tones activates both regions simultaneously; the regions may overlap if the difference in frequencies is relatively small (Fig. 1b). Finally, excitatory synaptic fields and the activated neuron clusters are modulated by inhibition (Fig. 1c). The mathematical basis for these computations is developed below. For clarity, only the main results are shown (details can be found in the supplementary material).

Neural Space

Although the brain has three spatial dimensions, only one dimension -that corresponding to the tonotopic axis- is relevant for a place code. Thus, the circular synaptic field in Fig. 1 is projected onto the tonotopic axis (bars). For simplicity, the neural space is defined as a single row of neurons (Fig. 2a). In the presence of sound, afferents from an external source generates a synaptic field that covers a contiguous subset of neurons (Fig. 2a). In the following, a mathematical description of the neural space will be developed that accommodates the neural elements and synaptic fields.

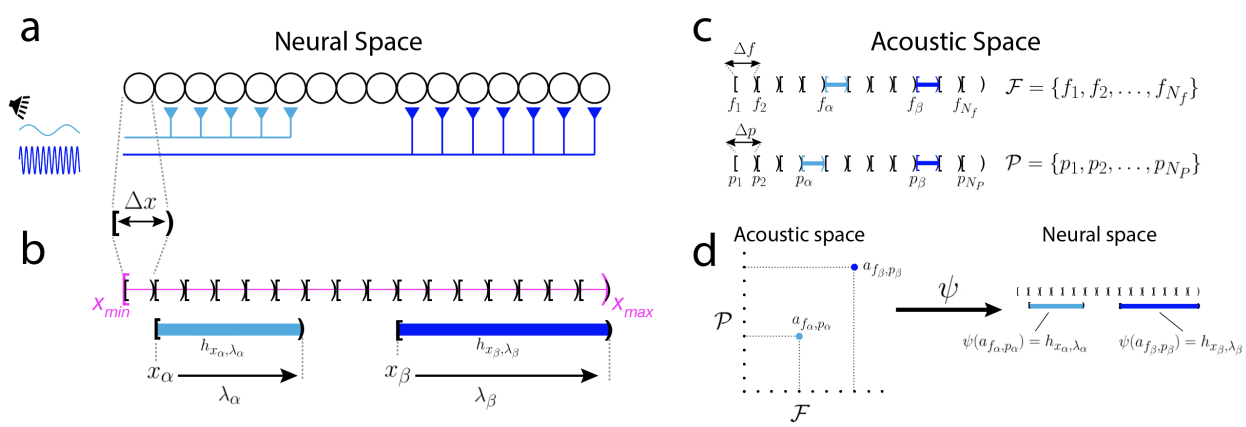

Figure 2: **Mathematical representation of neural and acoustic Spaces.** ***a***, neurons on the tonotopic axis are positioned next to each other with no space in between. Pure tone stimuli activate afferents onto a subset of neurons (cyan, blue). ***b***, mathematical representation of neural space. The tonotopic axis is a half-open interval (magenta) and is partitioned into smaller intervals that represent the space (Δx) taken up by neurons. The synaptic fields ($h_{x_\alpha,\lambda_\alpha}, h_{x_\beta,\lambda_\beta}$) are also half-open intervals. ***c***, The acoustic space has two dimensions, with frequency as one axis and pressure as the other. The frequency and pressure spaces are partitioned into half-open intervals of length $\Delta f, \Delta p$, respectively. ***d***, Mapping two tones in the acoustic space to intervals in neural space via the function ψ.

The neural space is taken to be an interval, bounded by minimum and maximum values x_{min} and x_{max} (Fig. 2b, magenta). To incorporate neurons, the neural space is partitioned into N_{cell} sections. Both the neural space and the cells are 'half-open' intervals, which are closed ("[") on one end and open on the other (")"). This is convenient mathematically because neurons can be packed next to each other with no space in between, allowing for a formal definition of a partition (see

supplementary material). Each neuron can therefore be expressed as the subinterval $[x, x + \Delta x)$, where Δx is the width of each neuron. Note that each neuron can be uniquely identified the point at the closed end, which also gives its location along the tonotopic axis. The set containing these points is:

$$\mathcal{X} = \{x_1, x_2, \ldots, x_{N_{cell}}\} \tag{1}$$

A synaptic field spans an integral number (n_λ) of neurons and is also a half-open interval with length $\lambda = n_\lambda \Delta x$. The length λ ranges from Δx (1 cell) to a maximum $\lambda_{max} = n_{max}\Delta x$. Each synaptic interval, designated as $h_{x,\lambda} = [x, x+\lambda)$, is uniquely identified by the location of the cell at the closed end (x_α, x_β in Fig. 2b) and by its length ($\lambda_\alpha, \lambda_\beta$). The set of starting points for synaptic intervals is a subset of $\mathcal{X}$:

$$\mathcal{X}_\lambda = \{x_1, x_2, \ldots, x_{N_\lambda}\} \subset \mathcal{X}; N_\lambda = N_{cell} - n_{max} \tag{2}$$

The set of all possible length λ values is :

$$\Lambda = \{\lambda_1, \lambda_2, \ldots, \lambda_{max}\} \tag{3}$$

As will be shown below, the set $\mathcal{X}_\lambda$ contains information about the frequency while the set Λ contains information about the sound pressure.

Mathematically, the set of all synaptic intervals in neural space is a basis for topology on $S_\mathcal{X}$, which is used to define algebraic operations and construct mapping from acoustic space (see below, supplementary material).

Representing sound in neural space

The elements of acoustic space $\mathcal{A}$ are pure tones, each of which is characterized by a sine wave of a given frequency (f) and amplitude corresponding to sound pressure (p). Theoretically, frequencies and sound pressures can take an uncountable number of values but physiologically, the audible range is bounded by minimum and maximum values. In addition, the resolution is limited in that tones with small differences in frequencies or sound pressures cannot be discriminated (frequency and intensity difference limens [8, 9, 10, 11]).

The acoustic space therefore has two dimensions with frequency as one axis and sound pressure as the other. As was done for neural space, the frequency axis is defined as a half-open interval delimited by minimum and maximum values: $[f_{\min}, f_{\max})$. It is further divided into N_f non-overlapping intervals, each of which is expressed as $[f, f + \Delta f)$ (Fig. 2c). Δf is the length of each interval and represents the minimum frequency difference that can be discriminated. For example, two tones with frequencies f_α, f_β that are in $[f_1, f_1 + \Delta f)$ will both be 'assigned' to f_1 (see supplementary material). Therefore, the audible and discriminable frequencies are given by the first points of each interval. The set containing these points is:

$$\mathcal{F} = \{f_1, f_2, \ldots, f_{N_f}\} \tag{4}$$

The set of audible sound pressures is constructed similarly:

$$\mathcal{P} = \{p_1, p_2, \ldots, p_{N_p}\} \tag{5}$$

The set has $N_{\mathcal{P}}$ half-open intervals of length Δp (Fig. 2c).

Features of the acoustic space are represented in neural space via a mapping ψ (Fig. 2d; see supplementary material for formal treatment). Note that a point in acoustic space ($a_{f,p}$) corresponds to the ordered pair (f, p) while an interval ($h_{x,\lambda}$) in neural space corresponds to (x, λ). Therefore, the mapping ψ is accomplished by first mapping the components f to x and p to λ via $\psi_f(f) = x$ and $\psi_p(p) = \lambda$.

$$\psi(a_{f,p}) = h_{\psi_f(f),\psi_p(p)} = h_{x,\lambda} \tag{6}$$

By adjusting the number of elements in each space appropriately ($|\mathcal{F}| = |\mathcal{X}_\lambda|$ and $|\mathcal{P}| = |\Lambda|$), the mapping becomes bijective (one-to-one,onto). Consequently, given an $h_{x,\lambda}$, it is possible to infer the tone $a_{f,p}$ via the inverse mapping $a_{f,p} = \psi^{-1}(h_{x,\lambda})$.

A mapping from acoustic space to intervals that are inhibitory can be similarly defined. The mapping is complicated by the fact that the number and receptive field properties of $\boldsymbol{E}$ and $\boldsymbol{I}$ cells differ. The mapping is under ongoing investigation but for purposes of the present analyses, the mapping is taken to be identical to that for $\boldsymbol{E}$.

Algebraic operations with synaptic intervals

Having formally described the mathematical structure of neural space, it is now possible to define the algebraic operations -addition and multiplication- for combining and modulating synaptic intervals (Fig.1b,c). An important condition that must be satisfied is that operations be 'closed'; that is, the result of adding and multiplying intervals remain within the neural space.

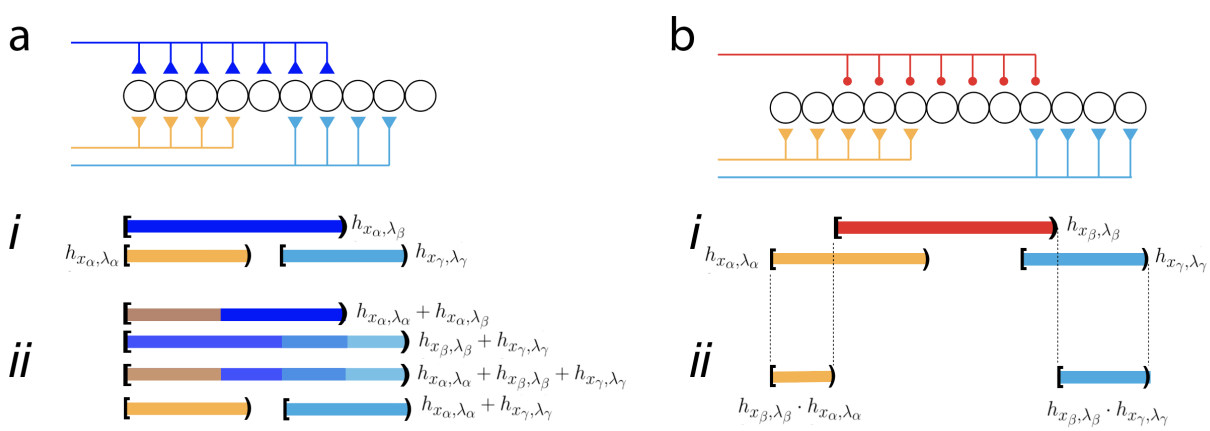

Figure 3: **Addition and Multiplication.** ***a***, schematic of network receiving three excitatory afferent inputs. ***i***, Synaptic intervals representing the synaptic fields. ***ii***, addition (union) of different combinations of intervals. **b**,schematic of network receiving two excitatory inputs (blue, cyan) and an inhibitory input (red). ***i***, synaptic intervals associated with the activated afferents. ***ii***, multiplication of two excitatory intervals (blue, cyan) by the inhibitory interval (red).

To satisfy closure, 'addition' of synaptic intervals is defined as the union. Let $h_{x_\alpha,\lambda_\alpha}, h_{x_\beta,\lambda_\beta}$ be two synaptic intervals. Then,

$$h_{x_\alpha,\lambda_\alpha} + h_{x_\beta,\lambda_\beta} \stackrel{\text{def}}{=} h_{x_\alpha,\lambda_\alpha} \cup h_{x_\beta,\lambda_\beta} \tag{7}$$

The addition operation yields two possible results (see supplementary materials for details). If the two synaptic intervals do not overlap ($h_{x_\alpha,\lambda_\alpha}, h_{x_\gamma,\lambda_\gamma}$ in Fig. 3a*i*), the union yields a set with the same two intervals (Fig. 3a*ii*, bottom). If the two intervals overlap ($h_{x_\alpha,\lambda_\alpha}+h_{x_\alpha,\lambda_\beta}, h_{x_\alpha,\lambda_\beta}+h_{x_\gamma,\lambda_\gamma}$), the result is a longer, single interval with starting point equal to the leftmost point and length that depends on the amount of overlap (Fig. 3a*ii*, top two traces). Note that if the starting points are the same (blue and orange intervals), the length of the resultant intervals are at most equal to that of longer summand, indicating that addition is sublinear.

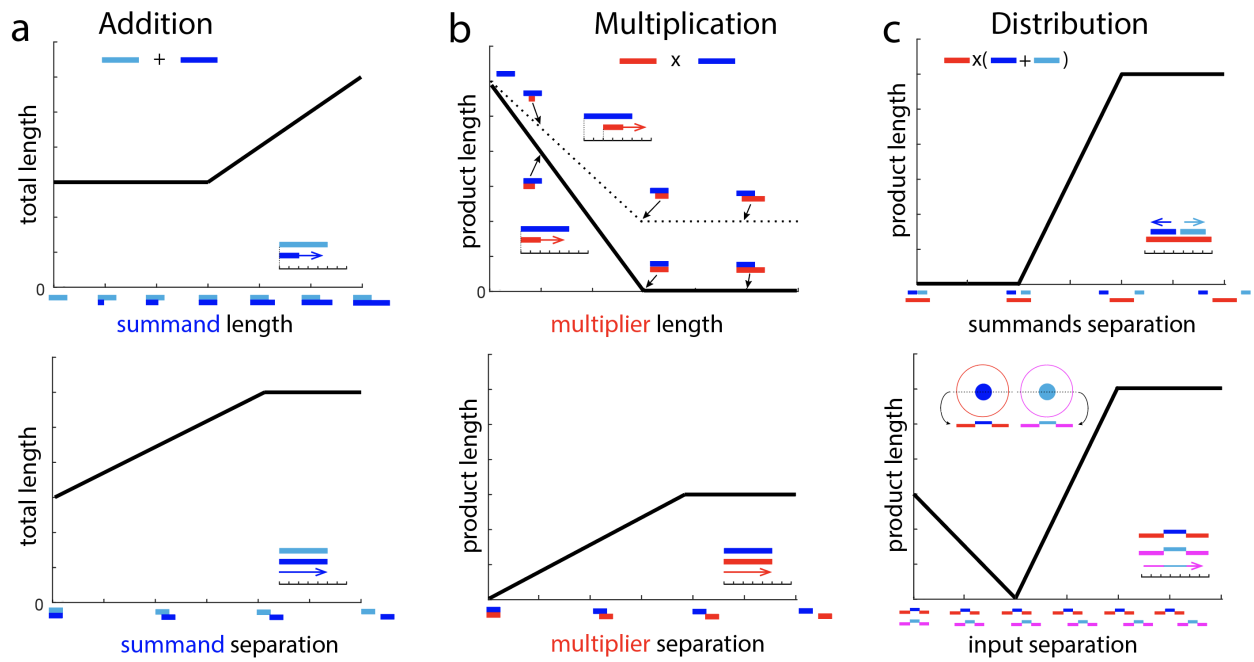

Figure 4: **Predicted effects of addition and multiplication**. ***a***, ***top***, addition of two intervals (cyan, blue) when the length of one interval (blue) is increased (top). ***Bottom***, one interval (blue) is shifted to the right of the other (cyan). ***b*, top**, multiplication of an excitatory interval (blue) by an inhibitory interval of increasing length (red) when the starting points of the intervals are the same (solid line) and when the inhibition is offset to the right of excitation (dotted line). ***c*, top**, effects of inhibition (red) on two excitatory intervals (blue, cyan). With the inhibitory interval at a fixed location, the distance between the excitatory intervals is increased systematically. ***Bottom***, Effects of two inputs configured as center-surround where the excitatory fields (blue, cyan) are flanked by inhibitory fields (red, magenta). One of the inputs is shifted systematically to the right of the other.

It is noteworthy that there is some ambiguity from a decoding perspective because the addition operation will fuse overlapping intervals into a larger, single interval (e.g. $h_{x_\alpha,\lambda_\beta}$ and $h_{x_\gamma,\lambda_\gamma}$ in Fig. 3a). It would not be possible, for example, to determine whether a long synaptic interval is a result of a single high intensity pure tone, multiple pure tones with small differences in frequencies, or band limited noise.

Closure is satisfied because the union of an arbitrary number of overlapping intervals results in an interval that is always within the neural space. The union of any number of disjoint sets is also within the neural space (more accurately, is a subset of the topology defined in $S_{\mathcal{X}}$, see supplementary material). A notable property that will be important later is that there is no additive inverse that can decrease the interval length.

One example of addition that occurs under biological conditions is when a pure tone arrives simultaneously to the two ears. The signal propagates separately through the auditory pathway but eventually converges at some brain region. Because a binaural input results from the same tone, the starting points of the synaptic intervals are the same, though the lengths may differ due to e.g. interaural intensity differences (orange and blue intervals in Fig. 3a). The predicted result of adding two intervals with different lengths is shown in Fig. 4a (top). Addition yields an interval length that is equal to the larger interval: the length is initially constant and equal to that of the cyan interval but then increases linearly when the length of the blue interval exceeds that of the cyan.

Addition also occurs if the sound is composed of two pure tones with different frequencies, which would generate two synaptic intervals with different starting points and possibly different lengths (e.g. orange and cyan intervals in Fig. 3a). The resulting length depends on the degree of overlap between the intervals. In Fig. 4a (bottom), the location of one interval (cyan) is fixed while the other of equal length (blue) is shifted rightward. When the two intervals completely overlap, the total length is equal to the length of one interval. As the blue interval is shifted, the total length increases linearly and plateaus when the two intervals become disjoint.

Inhibition decreases the excitability of the network and would be expected to reduce the size of the synaptic interval, which is not possible with the addition operation because there is no inverse (i.e. 'subtraction' is not defined). To incorporate the effects of inhibition, a 'multiplication' operation is introduced (Fig. 3b). For two synaptic intervals $h_{x_\alpha,\lambda_\alpha}, h_{x_\beta,\lambda_\beta}$, multiplication ('$\cdot$') of $h_{x_\alpha,\lambda_\alpha}$ by $h_{x_\beta,\lambda_\beta}$ is defined as:

$$h_{x_\beta,\lambda_\beta} \cdot h_{x_\alpha,\lambda_\alpha} \stackrel{\text{def}}{=} h_{x_\alpha,\lambda_\alpha} \setminus h_{x_\beta,\lambda_\beta} \tag{8}$$

The set minus operation "$\setminus$" eliminates the points from the multiplicand $h_{x_\alpha,\lambda_\alpha}$ that it has in common with the multiplier $h_{x_\beta,\lambda_\beta}$ (Fig. 3b*i,ii*) thereby decreasing its length. Note that this differs from the usual set theoretic definition of multiplication, where the product of sets is given by their intersection. Multiplication yields several results, depending on the relative locations and size of the multiplicand and the multiplier (see Supplementary material). Under biological conditions, the multiplier is an inhibitory ($\boldsymbol{I}$) interval and multiplicand ($\boldsymbol{E}$) is an excitatory interval. If the two intervals do not overlap, then the multiplicand is unaffected since they have no points in common. If the multiplier ($h_{x_\beta,\lambda_\beta}$) overlaps with the multiplicand ($h_{x_\alpha,\lambda_\alpha}$) and the starting point of the multiplier (x_β) is greater than that of the multiplicand (x_α), then the multiplicand is shortened. If the multiplicand is within the multiplier, the product is the empty set (i.e. complete cancellation). Other possible outcomes are detailed in the supplementary material.

Multiplication satisfies the closure property as the resulting interval is a half-open interval that is always in neural space. An important property is that multiplication is not commutative so that the order of operations matters: $h_{x_\beta,\lambda_\beta} \cdot h_{x_\alpha,\lambda_\alpha} \neq h_{x_\alpha,\lambda_\alpha} \cdot h_{x_\beta,\lambda_\beta}$. Other algebraic properties are discussed in the supplementary material.

If the excitatory and inhibitory inputs are co-activated during a tonal stimulus (as in feedforward circuits), then the $\boldsymbol{E}$ and $\boldsymbol{I}$ intervals will have the same starting points along the tonotopic axis. The length of the multiplicand after the operation (termed product length) depends on the relative

lengths of the multiplier and multiplicand (Fig. 4b, top). Increasing the multiplier length decreases the product length, becoming zero when it is greater than or equal to the length of the multiplicand (solid line). Differences in starting points can prevent full cancellation of the $\boldsymbol{E}$. If $\boldsymbol{I}$ is offset to the right of $\boldsymbol{E}$, increasing the $\boldsymbol{I}$ interval length causes the product interval to plateau to non-zero, constant value equal to the offset (**b**, dashed line).

If the $\boldsymbol{E}$ and $\boldsymbol{I}$ inputs are independent of each other, the synaptic intervals may occur at disparate locations along the tonotopic axis. Figure 4(b,bottom) shows the predicted effects on product length when the starting point of inhibition (red) is shifted systematically to the right of the excitation (blue). The product length is least when there is maximal overlap between the two intervals and increases linearly as the overlap decreases, eventually plateauing to a constant value when the intervals become completely disjoint.

With addition and multiplication defined, the rules for combining the two operations can now be determined. A simple, hypothetical scenario is when a network receives two excitatory inputs that results in synaptic intervals $(h^E_{x_\alpha,\lambda_\alpha}, h^E_{x_\beta,\lambda_\beta})$ and a single inhibitory input that result in an inhibitory interval $(h^I_{x_\gamma,\lambda_\gamma})$. When all three inputs are activated simultaneously, the intervals combine in neural space as $h^I_{x_\gamma,\lambda_\gamma} \cdot (h^E_{x_\alpha,\lambda_\alpha} + h^E_{x_\beta,\lambda_\beta})$. It can be shown that multiplication is *left* distributive so that (see supplementary material):

$$h^I_{x_\gamma,\lambda_\gamma} \cdot (h^E_{x_\alpha,\lambda_\alpha} + h^E_{x_\beta,\lambda_\beta}) = (h^I_{x_\gamma,\lambda_\gamma} \cdot h^E_{x_\alpha,\lambda_\alpha}) + (h^I_{x_\gamma,\lambda_\gamma} \cdot h^E_{x_\beta,\lambda_\beta}) \tag{9}$$

Intuitively, this means that the effect of a single inhibitory input on two separate excitatory inputs may be calculated by computing the inhibitory effects on each input separately and then adding the results.

Multiplication, however, is not *right* distributive. Thus, given two inhibitory intervals ($h^I_{x_\alpha,\lambda_\alpha}$ and $h^I_{x_\beta,\lambda_\beta}$) acting on a single excitatory interval $(h^E_{x_\gamma,\lambda_\gamma})$:

$$(h^I_{x_\alpha,\lambda_\alpha} + h^I_{x_\beta,\lambda_\beta}) \cdot h^E_{x_\gamma,\lambda_\gamma} \neq (h^I_{x_\alpha,\lambda_\alpha} \cdot h^E_{x_\gamma,\lambda_\gamma}) + (h^I_{x_\beta,\lambda_\beta} \cdot h^E_{x_\gamma,\lambda_\gamma}) \tag{10}$$

The result of multiplication depends on the degree of overlap between the intervals and relative locations. In Fig. 4 c (top), the locations of two excitatory intervals (blue, cyan) is shifted left- and rightward relative to an inhibitory interval (red). Initially, the two $\boldsymbol{E}$ intervals are completely within the $\boldsymbol{I}$ interval so the product length is zero. When the two $\boldsymbol{E}$ intervals reach the borders of the $\boldsymbol{I}$ interval, the product length increases and reaches a plateau when the $\boldsymbol{E}$ and $\boldsymbol{I}$ intervals become disjoint.

A common physiological scenario is when sound is composed of two pure tones and each tone results in an excitatory synaptic field surrounded by an inhibitory field (center surround inhibition, inset in Fig. 4c, bottom), see also inset in Fig. 8b, *iii*). Letting the $\boldsymbol{E}$ -$\boldsymbol{I}$ interval pair for one pure tone be h^E_α, h^I_α and that for the other be h^E_β, h^I_β, the mathematical expression describing the computation is:

$$(h^I_\alpha + h^I_\beta) \cdot (h^E_\alpha + h^E_\beta) \tag{11}$$

An important consequence of the distributive properties of multiplication (left but not right distributive over addition) is that eq. 11 is not equivalent to multiplying each excitatory interval by its associated interval first and then adding the results:

$$(h^I_\alpha + h^I_\beta) \cdot (h^E_\alpha + h^E_\beta) \neq (h^I_\alpha \cdot h^E_\alpha) + (h^I_\beta \cdot h^E_\beta) \tag{12}$$

The exceptions to eq. 12 are when there are no overlaps between the excitatory $(h^E_\alpha \cap h^E_\beta = \emptyset)$ and inhibitory $(h^I_\alpha \cap h^I_\beta = \emptyset)$ intervals.

Simulations with spiking neurons

Key features of the mathematical model were examined with simulations of spiking neurons in a 2-dimensional network of excitatory and inhibitory neurons [24]. Both ***E*** and ***I*** neurons receive a Gaussian distributed excitatory drive from an external source (Fig. 5a, bottom; blue disk in middle and top); the ***E*** cells in addition receive feedforward inhibitory inputs from the ***I*** cells (red disk in top). The recurrent connections between neurons were omitted because previous simulations with experimentally-determined parameters [25] indicated that the recurrent connections contribute minimally to the firing in auditory cortical circuits [24]. The brief stimulus (50 ms) elicited a single action potential in neurons within the synaptic field (dots in Fig. 5b, top). The region encompassing active neurons (henceforth termed activated area; (Fig. 5b, top) was quantified by fitting a circle (magenta) to the outermost points. The underlying synaptic field was taken to be the portion of the total current that exceeded (more negative than) rheobase, the minimum current needed to evoke an action potential (I_{Rh} in Fig. 5b, bottom) and quantified either as the diameter of a circle fitted to the outermost boundary with a circle (magenta) or the projection to one axis (orange bar). Note that the spatial dimensions has units of cell number (see Methods).

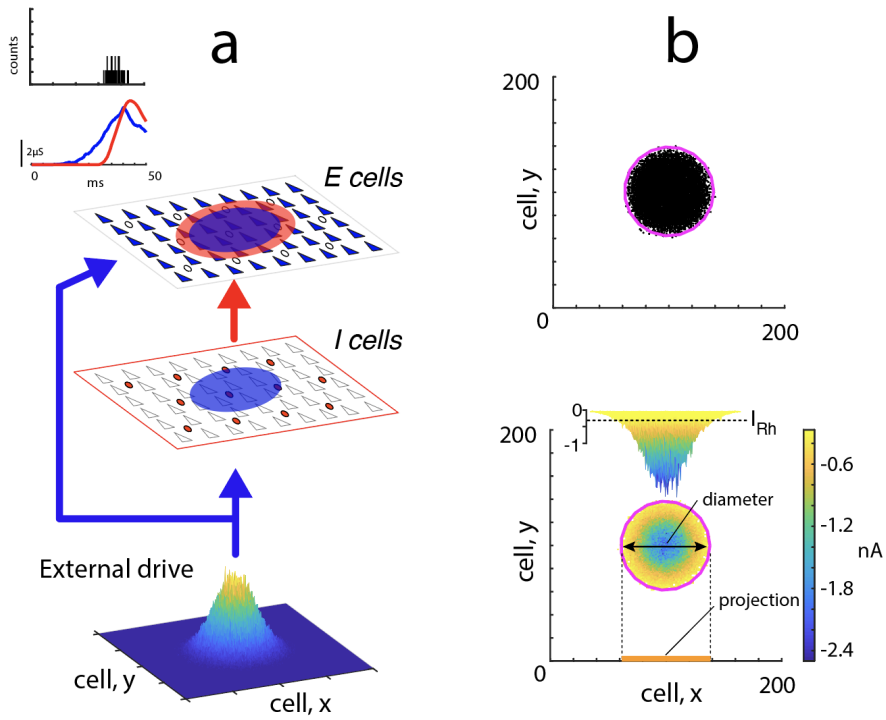

Figure 5: **Simulations with spiking neurons.** ***a***, schematic of two-dimensional network. ***Inset***, excitatory (blue) and inhibitory (red) conductances evoked in a cell and poststimulus time histogram of spikes (black). ***b, bottom***, composite current obtained by summing excitatory and inhibitory synaptic currents. The spatial extent of the current (termed synaptic field) is quantified by thresholding with rheobase (I_{Rh}), fitting the perimeter with a circle (magenta), and calculating either its diameter or the length of its projection on one axis. ***top***, action potentials triggered in cells within the synaptic field.

To test the addition operation (Fig. 4), two external excitatory stimuli were delivered to the

center of the network simultaneously (without inhibition). Increasing the width of one stimulus ($\sigma_\alpha : 2 - 45$ cells), while keeping that of the other fixed at $\sigma_\beta = 20$ cells, increased the diameters of the total synaptic field and activated areas (Fig. 6a, top, *i-iii*). As predicted (bottom), the diameters of the synaptic field (orange) and activated area (black) initially did not change when σ_α was smaller than σ_β ($\frac{\sigma_\alpha}{\sigma_\beta} < 0.5$) but then increased as σ_α continued to widen. However, because the synaptic currents were Gaussian distributed (Fig. 5b, bottom), the curve started increasing before σ_α became equal to σ_β ($\frac{\sigma_\alpha}{\sigma_\beta} = 1$). When delivered simultaneously, the magnitude of the resultant current also increased in Fig 6 a, top), causing the region that exceeded rheobase to widen (compare synaptic fields in *i* with *ii*). The diameter is proportional to the standard deviation when two Gaussian distributions sum (diameter $\propto \sqrt{\sigma_\alpha^2 + \sigma_\beta^2}$, not shown).

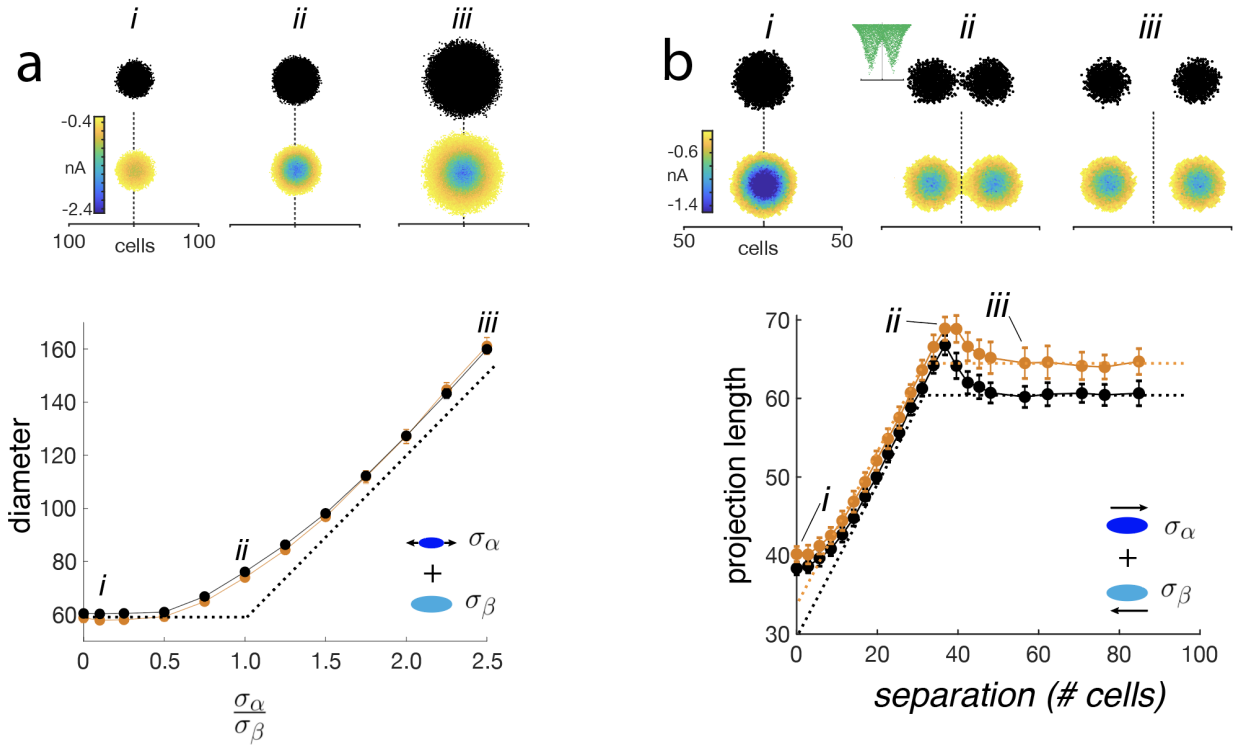

Figure 6: **Test of addition.** ***a, top***, Activated area (top; 1 sweep) and underlying synaptic field (bottom; average of 25 sweeps). ***i***, one stimulus. ***ii-iii***, two stimuli delivered to the center of the network. The diameter (σ_α) of one input was systematically increased while that of the other (σ_β) was kept constant. ***Bottom***, plot of synaptic field (orange) and activated area (black) diameters vs $\frac{\sigma_\alpha}{\sigma_\beta}$. Dashed curve is predicted relation ***b*** addition of two spatially separated excitatory inputs. ***top***, activated areas and synaptic fields with increasing stimulus separation. (***i - iii***). Inset in ***ii*** shows example of excitatory synaptic current profiles. ***Bottom***, projection length vs. separation distance for synaptic field (orange) and activated area (black). Dashed curves are predicted changes.

To examine the addition of spatially disparate synaptic fields, two excitatory inputs were delivered at different distances from each other (Fig. 6b, top). Consistent with the prediction (bottom), the projection length of the synaptic field (orange) and activity areas (black) increased with stimulus separation and reached a plateau when the two inputs became fully disjoint (***iii***). The diameters were greater than predicted (dashed lines) when the separation was small (< 10 cells) and when the intervals are just becoming disjoint (at separation ~ 40 cells, ***ii***). As discussed above, the

deviation was because the inputs were Gaussian distributed. At separations of 30-40 cells, the two synaptic fields 'fused' together and increased the projection length (top, ***iii***).

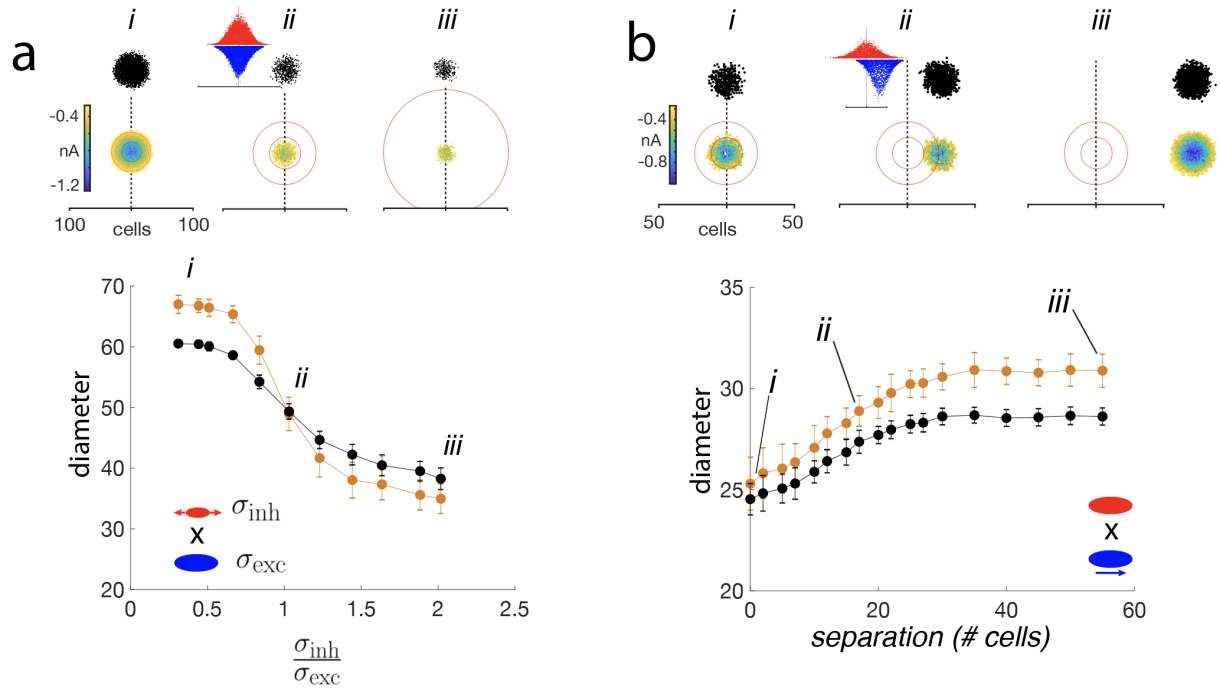

Figure 7: **Test of multiplication.** ***a, top, i-iii*** activated areas and synaptic fields evoked with excitatory and inhibitory inputs. The spatial extent of the inhibition is demarcated by the red circles (inner circle: 1 σ_{inh}; outer: 2 σ_{inh}). Inset in ***ii*** shows an example of excitatory (blue) and inhibitory (red) synaptic current profile. ***Bottom***, plot of activated area (black) and synaptic field (orange) vs $\frac{\sigma_{inh}}{\sigma_{exc}}$. ***b***, Same as in ***a*** except that the excitatory input was shifted systematically to the right of inhibition. ***Bottom***, Diameters of activated area (black) and synaptic field (orange) plotted against separation between excitatory and inhibitory synaptic fields

.

To test the multiplication operation, the ***E*** and ***I*** neurons were stimulated simultaneously, resulting in excitatory (blue, inset of Fig. 7 a, *ii*) and inhibitory (red) synaptic fields. The width (σ_{exc}) of the excitatory synaptic field was kept constant while that (σ_{inh}) of the inhibitory field was increased systematically (red circles delimit σ_{inh} and $2 \times \sigma_{inh}$). As predicted, the diameter of the synaptic field decreased with increasing σ_{inh} (Fig. 7a, bottom). However, the diameter asymptoted towards a non-zero constant. The excitatory synaptic field was not canceled completely even when the inhibition was twice as wide (top, ***iii***). Because the network was feedforward, the inhibitory input was delayed relative to excitation by about 10-15 ms (Fig. 5a, inset); as a result, there was always a time window where excitation dominated. The result is better predicted by the math model when there is an offset in the starting location of inhibition, as in Fig. 4 (top, dashed line).

To examine multiplication of spatially disparate ***E*** and ***I*** fields, the excitatory input was shifted systematically to the right of the inhibitory input (Fig. 7b). As predicted, the product length increased with the ***E*** -***I*** separation, although again, the length was not zero when the two completely overlapped (separation = 0 cells).

To examine how multiplication distributes over addition, two excitatory and one inhibitory inputs were delivered simultaneously to the network, resulting in two excitatory fields (h^E_α, h^E_β) and

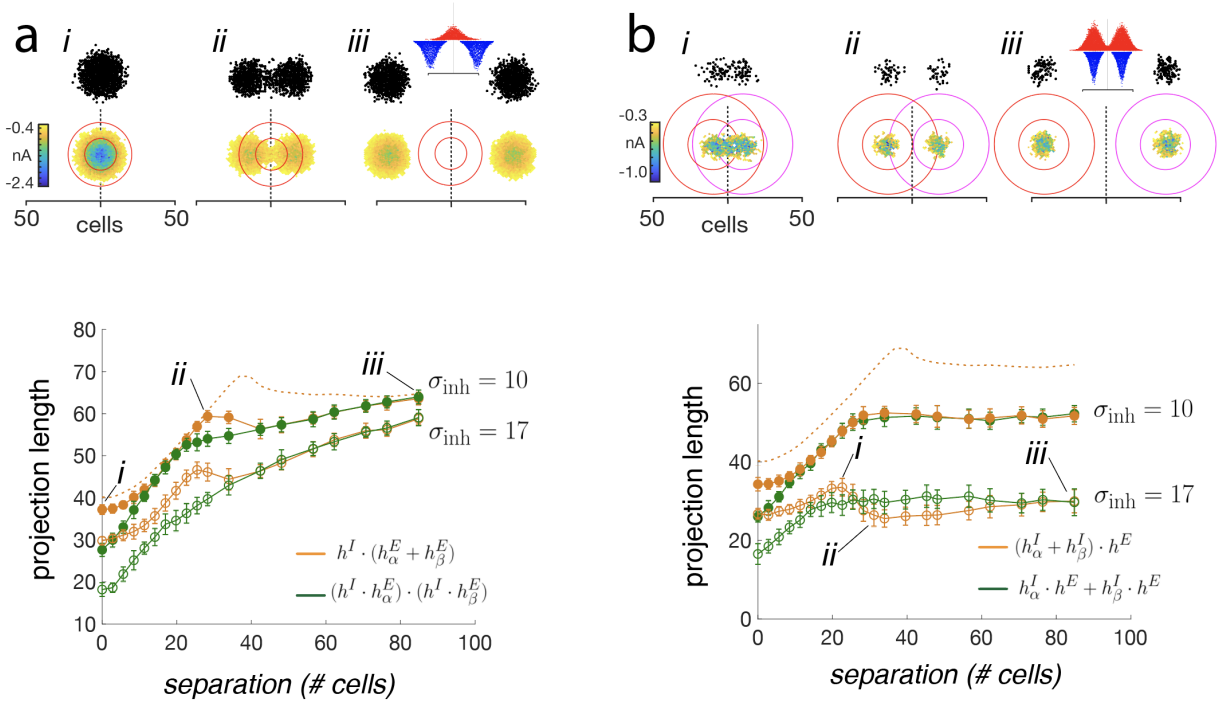

Figure 8: **Test of distributive properties.** ***a, top, i-iii*** Representative activated areas and synaptic fields generated by two excitatory inputs and a single inhibitory input. With the location of inhibition fixed, the two excitatory inputs ($\sigma_{exc} = 10$) were separated systematically. The spatial extent of the inhibition is demarcated by the red circles (inner circle: 1 σ_{inh}; outer: 2 σ_{inh}). Inset in ***iii*** shows the excitatory (blue) and inhibitory (red) synaptic current profile. ***Bottom***, plot of projection lengths (orange) vs separation of the excitatory inputs. Closed symbols: $\sigma_{inh} = 10$; Open symbols: $\sigma_{inh} = 17$. Green symbols are projection lengths obtained when inhibition was co-stimulated first with one excitatory input and then with the other and their projection lengths summed. Dotted curve is with no inhibition. ***b***, Simulations with two excitatory-inhibitory pairs, each with center-surround configuration (inset in ***iii***). ***Bottom***, Legend as in ***a*** except that the green traces plot the projected lengths obtained when each ***E*** - ***I*** pair were delivered separately and the individual projection lengths summed.

one inhibitory field (h^I; Fig. 8a). This is equivalent mathematically to $h^I \cdot (h^E_\alpha + h^E_\beta)$. All three inputs were initially at the center (***i***) and then with the inhibition stationary, the two excitatory inputs were shifted left and right (Fig. 8a, *i-iii*). As predicted (Fig. 4 c, top), the projection length increased as the excitatory fields moved away from inhibition (orange curves, bottom). To reproduce $h^I \cdot h^E_\alpha + h^I \cdot h^E_\beta$, simulations were performed with inhibition, first with one of the excitatory inputs and then with the other; the resultant projection lengths of each were then summed (green, Fig. 8a, bottom). The results of the two stimulus conditions matched when the separation between the excitatory inputs were $>$ 50 cells. The match was poor at smaller separation due to the summation properties of the Gaussian distributed currents (see above).

Finally, to examine the interaction of inputs with center-surround inhibition (Fig. 4c, bottom), two excitatory inputs, each with associated inhibitory fields were delivered to the network (inset in Fig, 8 (top, ***iii***) at different distances from each other. When the inhibitory field was wider than the excitatory field (lateral inhibition configuration, $\sigma_{inh} = 17, \sigma_{exc} = 10$; open orange circles in Fig. 8b, bottom), the projection length decreased (separation $>$ 20 cells; (*ii*)) and then increased to a plateau (*iii*). However, contrary to predictions, the length increased when the separation was less that 20 cells, likely due to the interaction of the Gaussian distributed excitatory fields (see above).

To confirm that the same result could not be obtained by presenting each stimulus separately ($(h^I_\alpha + h^I_\beta) \cdot (h^E_\alpha + h^E_\beta) \neq (h^I_\alpha \cdot h^E_\alpha) + (h^I_\beta \cdot h^E_\beta)$) (eq. 12), each ***E -I*** pair was delivered separately and the individual projection lengths summed. Unlike with simultaneous stimulation, the projection lengths increased monotonically and then plateaued without the dip (open green circles). The match was better for the co-tuned configuration ($\sigma_{inh} = \sigma_{exc} = 10$) because the inhibition was too narrow to produce a dip in the curve (filled orange vs filled green).

Discussion

The aim of this study was to develop a mathematical framework for a place-code and derive the underlying principles for how tones of varying frequencies and intensities are represented, assembled, and modulated in networks of excitatory and inhibitory neurons. The model is not intended to replicate the detailed dynamics of biological networks but rather to provide a 'skeleton' to aid in the interpretation of experimental data and the construction of computer simulations.

Key findings are as follows (detailed below). First, the 'functional unit' of neural space is a set of contiguous neurons that have flexible borders. The associated mathematical architecture, or topology, is a collection of half-open intervals. Pure tones are encoded solely by the location and length of the intervals, without the need for firing rate or timing information. Second, the architecture dictated the range and resolution of tone frequencies and intensities that can be represented in neural space. Finally, computations in neural space for combining and modulating units are addition (union) and multiplication (set minus). The associated algebraic laws limit the type of operations that can be performed on the intervals.

Significance and Implications

In order to encode both frequency and intensity, the 'functional' units in the model have flexible borders that can expand, unlike classical cortical columns [17]. Each is a contiguous set of neurons that receive tone-evoked synaptic inputs (synaptic field). Encoding sound involves mapping a point in acoustic space (pure tone with frequency f and pressure p) to an element in neural space (interval at location x with length λ). It is noteworthy that a tone is in effect represented by a population of

neurons and it is not possible to decode the tone frequency or intensity from the firing of a single neuron.

The algebraic operations determine the computations that can be performed with a place code. An important property for addition and multiplication is that the results remain within the neural space (closure property). This would not be true, for example, if addition is defined as the standard sum of the interval lengths ($|h_\alpha|+|h_\beta|$) because the result could exceed the boundaries of the neural space if each interval is too long or located near the edge of the tonotopic axis. Similarly, defining the effect of inhibition as subtraction ($|h^E|-|h^I|$) could produce negative intervals. These difficulties were avoided by defining addition as the union and multiplication as the set difference operation. Compared with the more familiar vector space, the number of allowable computations is relatively limited (see supplementary material); many of the linear algebraic operations used commonly for analyses and computational models are not permitted.

One implication of defining addition as the union is that if two intervals overlap ($h_\alpha \cap h_\beta \neq \emptyset$), the length of resulting interval (h_γ) is always less than the linear sum of lengths of the summands ($|h_\gamma| < |h_\alpha| + |h_\beta|$). If the starting points are the same ($x_\alpha = x_\beta$), as would occur during binaural stimulation, the resulting interval is equal to that of the longer summand ($|h_\alpha|+|h_\beta| = |h_\alpha|$, $|h_\alpha| \geq |h_\beta|$). Indeed, in the inferior colliculus, the response evoked with binaural stimulation is equal to that evoked with stimulation of only the contralateral ear, which evoked a larger response than stimulation of the ipsilateral ear [26] (see Figure in supplemental material). Assuming that loudness perception is related to the length of synaptic intervals, a possible psychophysical analog is that a tone presented binaurally is perceived to be less than twice as loud as monaural stimulation [27]. In both examples, the apparent sublinear effects arises from the properties of addition operation, though the effect may be enhanced by inhibition.

The distributive properties suggest how multiple excitatory inputs can be modulated by multiple inhibitory inputs. The effect of inhibition acting on two excitatory intervals (e.g. modulation of convergent binaural inputs by local inhibitory interneurons) can be predicted by examining the effects of inhibition on each interval separately and then summing the lengths (eq. 9; see below for caveats). However, this is not true for two sources of inhibition acting on a single excitatory interval (eq. 10). In cortical circuits, for example, excitatory neurons can be innervated by several classes of inhibitory interneurons [28]. The model suggests that accurately determining the overall effect of inhibition requires that the inhibitory interneurons be stimulated simultaneously; estimating the effect by sequential stimulation of each inhibitory inputs is generally incorrect.

The model shows that an inherent problem with the place coding scheme is that it is not possible to completely decode features of multi-component sound stimulus. Although the mapping from acoustic space to neural space is bijective, some ambiguities arise when a sound consists of tones with similar frequencies and/or high pressure levels. In neural space, there is a greater likelihood that the intervals fuse into fewer intervals (i.e. union of overlapping intervals). Hence, it is not possible to determine whether a long, contiguous synaptic interval is due to a single high intensity pure tone, multiple low intensity pure tones that have small differences in frequencies, or a bandwidth limited noise stimulus. Mathematically, the addition operation is a mapping from a two dimensional space to a one dimensional space (see supplementary material). The problem is akin to finding the combination of integers that sum to 10. The ambiguity appears to be manifested in psychophysical experiments: subjects perceive tones with small differences in frequencies as a single, louder tone [29] and have difficulties distinguishing the individual components of a multi-frequency stimulus [30, 31].

Although the model was developed for networks, it may apply generally to other aspects of auditory neuroscience. A well-documented phenomenon in auditory psychophysics is that perceived loudness of two tones presented simultaneously does not increase until the frequency difference

exceeds a 'critical band' [32, 33]. Assuming that loudness perception is related to the length of synaptic interval, this phenomenon may be expressed mathematically as $h_\alpha + h_\beta + h_{CB}$, where h_α, h_β represent the intervals generated by two tones and h_{CB} is the 'interval' of the critical band. Hence, $|h_\alpha + h_\beta + h_{CB}| = |h_\alpha \cup h_\beta \cup h_{CB}| = |h_{CB}|$ if $h_\alpha, h_\beta \subset h_{CB}$ but starts increasing when either intervals fall outside the critical band, much like Fig. 4a, top.

Finally, the mathematical architecture sets up the rules for transmitting information across brain regions. With the topologies and algebraic structures of neural networks known, it is possible with standard mathematical techniques to determine whether the mapping between neural spaces is e.g. continuous and bijective and whether the operations are preserved. Conversely, it is also possible to determine the optimal topology of the target or recipient space that would produce a desired mapping. In this study, for example, the structure of the acoustic space needed to create a bijective, continuous mapping to neural space was derived from the topology of the neural space.

Assumptions and limitations

The mathematical model was conditioned on two salient features of the auditory system. One is that the neural space is tonotopically organized. Tonotopy has been described in most neural structures in the auditory pathway, from brainstem areas [4, 34, 35] to at least layer 4 of primary auditory cortex. Whether tonotopy is maintained throughout cortical layers is controversial, with some studies (all in mice) showing clear tonotopy [36, 37, 38, 39] and others showing a more 'salt-and-pepper' organization [40, 41, 39]. A salt-and-pepper organization suggests that the incoming afferents are distributed widely in the neural space rather than confined to a small area. The model requires a relatively prominent tonotopy to satisfy the requirement that synaptic intervals encompass a contiguous set of cells.

A second condition is that the size of the synaptic interval and activated area increases with the intensity of the sound. Intensity-related expansion occurs in the cochlea [21, 22, 42] and can also be inferred from the excitatory frequency-response areas (FRAs) of individual neurons. The FRAs, which reflect the firing of cells to tones of varying frequencies and intensities, are typically "V-shaped". At low intensities, neurons fire only when the frequencies are near its preferred frequency (tip of the V). At higher intensities, the range of frequencies that trigger action potentials increases substantially [43, 37]. If adjacent neurons have comparably-shaped FRAs but with slightly different preferred frequencies, an increase in intensity would translate to an increase in the spatial extent of activated neurons.

The algebraic operations were derived from set theoretic operations and the magnitude of the underlying synaptic inputs were irrelevant. Under biological conditions, the input magnitude determines the degree to which biophysical, synaptic, and network processes become engaged and will affect the length of the synaptic intervals and activated areas. Not surprisingly, the results of the network simulations deviated quantitatively from the mathematical predictions in some regimes (compare Fig. 4 to Figs 6,7). Most of the discrepancies in the simulations were because the magnitudes of the synaptic inputs were Gaussian distributed along the tonotopic axis (see main text). In biological networks, the discrepancies may be exacerbated by the presence of threshold processes such as regenerative events [44, 45]. Though the algebraic operations remain valid overall, they may be obscured in regimes such as these.

The model incorrectly assumes that the strength of inhibition is sufficiently strong to fully cancel excitation. This facilitated analysis because the effect of multiplication depends solely on the overlap between the multiplicand and multiplier. As the simulations with the feedforward network showed, the excitation cannot be fully canceled by inhibition owing to synaptic delay. Moreover, the balance is spatially non-homogeneous: in center-surround suppression, excitation

dominates at the preferred frequency with inhibition becoming more prominent at non-preferred frequencies [43, 46, 47]. To apply multiplication to biological systems, it may be necessary to define empirically an "effective" inhibition. For example, the data in Fig. 7a match the prediction better if inhibition is offset relative to excitation (Fig. 4b,top).

Application to experiments

The functional unit was defined as the synaptic interval rather than the activated area, which reflects the number of neurons that actually fired. This facilitated mathematical analyses because a contiguous set of neurons could be defined (not all neurons within the synaptic field fired so there were pockets of inactive cells) and also because multiplication by inhibitory synaptic intervals could be more easily incorporated into the mathematical framework. Though measuring the intracellular potentials of a large population of cells is currently not feasible experimentally, the extent of the synaptic field may be estimated from the activated area (Figs. 5,6,7,8), which can be measured with imaging techniques.

For mathematical convenience, the location of the synaptic intervals was identified by the leftmost point (closed end) of the interval with increases in intensity signaled by a lengthening of the interval in the rightward (high frequency) direction. Surprisingly, similar behavior has been observed in the cochlea albeit in the opposite direction: an increase in the intensity causes a shift towards low frequency region of the basilar membrane while the high frequency cutoff remains fixed [42, 22, 3]. The choice of the leftmost point to tag the interval is arbitrary and any point in the interval will suffice provided an analogous point can be identified in each interval in the set. Experimentally, using the center of mass of active neurons as the identifier might be more practical.

As discussed above, there are likely regimes where the algebraic operations may be obscured. By the same token, there are regimes where the algebraic laws may be technically violated but the results are sufficiently good for practical purposes. For example, if the excitation and inhibition have comparable widths (Fig. 8b), the interactions between two center surround inputs can be estimated accurately by sequential activation of each input even though it is mathematically improper. Experimentally, it will be necessary to explore a range of stimulus conditions to determine the regimes where the analyses are valid and/or can be relaxed.

Alternatives to interval-based place code

As discussed above, a shortcoming of the interval-based place code is the fusion of intervals that can occur when the sound has multiple tonal components, leading to ambiguities in decoding. In principle, this problem may be mitigated by re-defining the neural space so that the functional elements are non-overlapping clusters of neurons, similar to the classical cortical column [17] (see supplemental material). For this model, frequency is encoded by the location of the columns and sound pressure by the number of neurons that fire within a column (the stimulus is assumed brief so that neurons are binary units). The result is that the units remain separate regardless of the number of tonal components. A major disadvantage, however, is that it is difficult to encode a large frequency range without compromising the number of pressure levels that can be represented. To maximize the number of frequency levels, the number of columns should be large, which means that the column size should be as small as possible; the converse is needed to maximize the number of pressure levels.

Another alternative is a purely combinatorial code [48, 49], where coding sound features is based on which combination of neurons are activated, without reference to their location or rate. The main advantage is that the number of possible features (for binary neurons) that can represented

is potentially very large (2^n, n = number of neurons). Ambiguities in representing multiple tones could be conceivably be avoided if there many neurons. However, this means that the 'look-up' table for decoding all the possible combinations of activity patterns is also very large. Moreover, without some organizing principle, it may be more difficult to define mappings between acoustic space and neural space and between different brain regions. An advantage of being able to describe the mathematical architecture (topology) is that mapping between spaces is more easily formulated using standard mathematical techniques.

Methods

Simulations were performed with a simplified version of a model of the auditory cortex [24]. The model is 200 x 200 cell network composed of 75% excitatory ($\boldsymbol{E}$) and 25% inhibitory ($\boldsymbol{I}$) neurons (Fig. 5), spaced approximately 7.5 μ apart. The neurons are adaptive exponential integrate-and-fire units with parameters adjusted to mimic excitatory pyramidal and fast spiking inhibitory neurons [25]. The spatial connection profiles between neurons were based on experimental data [25]. Both cell types received excitatory external drive that represents thalamic input (Fig. 5a, bottom); blue in middle, top). The magnitude of the external drive was Gaussian distributed (Fig. 5a, bottom); the magnitude and spatial extent was varied by changing the amplitude and standard deviation. The synaptic inputs to each cell lasted 50 ms so that cells fired a single action potential. The magnitudes were randomized so that the synaptic fields and activated areas varied from trial to trial. When activated, the $\boldsymbol{I}$ cells generated inhibitory currents in the $\boldsymbol{E}$ cells within a confined area (top, red). The network therefore has a feedforward inhibitory configuration. For some simulations, the $\boldsymbol{E}$ and $\boldsymbol{I}$ cells received separate external, excitatory drive they could be varied independently. The width of the inhibition was varied by changing the width of the external drive.

The spatial extent of the synaptic input was quantified from the circumference of the rheobase, the minimum current needed to evoke an action potential in the $\boldsymbol{E}$ cells (I_{Rh} inset in Fig. 5b, bottom). Rheobase is approximately -0.27 nA. The net synaptic current near firing threshold (V_θ) was calculated as $I_{\text{net}} = g_{exc} * (V_\theta - E_{exc}) + g_{inh} * (V_\theta - E_{inh})$ where g_{exc}, g_{inh} are the excitatory and inhibitory conductances, respectively, and $E_{exc} = 0$ mV, $E_{inh} = -80$ mV are the associated reversal potentials. The synaptic field is then defined as the area of the network where the total current exceeded (more negative than) I_{Rh} (Fig. 5,b). The circumference of the synaptic field was estimated by fitting the outermost points with a circle (maroon circle in Fig. 5b, bottom), after which the diameter could be measured. For stimuli with multiple components, the spatial extent was quantified as the total length of the projection onto the tonotopic axis. For all plots, the data points are mean +/- standard deviation.

Acknowledgements

I thank L-S Young and A. Bose for reading the manuscript and providing helpful comments. This work was supported by DARPA- Lifelong Learning Machines

Supplementary material

Acoustic Space

The general approach for defining acoustic space is as follows. The elements of acoustic space are pure tones of varying frequencies and sound pressures. It is therefore a product of frequency space $S_{\mathcal{F}}$ and pressure space $S_{\mathcal{P}}$: $S_{\mathcal{A}} = S_{\mathcal{F}} \times S_{\mathcal{P}}$. Biologically, the range of audible and discriminable frequencies and sound pressures are limited. To reflect this, the frequency and pressure spaces will each be defined as a topological space where the underlying set is an interval but the topology is coarser than the usual topology.

The frequency space ($S_{\mathcal{F}}$) is defined as a half-open interval on the positive real line: $S_F = [f_{min}, f_{max}) \subset \mathbb{R}^+$, where f_{min}, f_{max} are the minimum and maximum audible frequencies, respectively. To account for the fact that discriminability is limited (i.e. tones of similar frequencies are perceived as the same), $S_{\mathcal{F}}$ is divided into N_f half-open intervals $h_f = [f_\alpha, f_\beta) = [f_\alpha, f_\alpha + \Delta f)$ where $\Delta f = \frac{1}{N_f}$ is the length of the interval and represents the minimum frequency difference that can be discriminated. The use of half-open intervals ensures that there is no 'gap' between adjacent frequency intervals. The set of all half-open intervals is:

$$\begin{aligned} \mathcal{H}_{\mathcal{F}} &= \{h_{f_i} = [f_i, f_i + \Delta f), f_i \in S_{\mathcal{F}}, f_i \leq |S_{\mathcal{F}}| - \Delta f\} \\ &= \{h_f = [f_{min} + i\Delta f), f_{min} + (i+1)\Delta f) \mid i \in \mathbb{N}_0, i < N_f\} \end{aligned} \tag{13}$$

The topology $\tau_{\mathcal{F}}$ is generated by the elements of $\mathcal{H}_f$:

$$\tau_{\mathcal{F}} = \{\bigcup H_f \mid H_f \subseteq \mathcal{H}_{\mathcal{F}}\} \tag{14}$$

The set of intervals is a partition where each interval is an equivalence class $[f_j]$: for $f_\alpha, f_\beta \in S_F, f_\alpha \sim f_\beta$ if $f_\alpha, f_\beta \in [f_i, f_i + \Delta f)$. This may be extended so that $f_\alpha \sim f_\beta$ if $f_\alpha, f_\beta > f_{max}$ and $f_\alpha \sim f_\beta$ if $f_\alpha, f_\beta \leq f_{min}$. Frequencies f_α, f_β are 'assigned' to f_i if they are between f_j and $f_j + \Delta f$. Thus, f_α, f_β are indistinguishable from each other since both are classified as f_i. Each frequency interval is uniquely identified by the minimum point at the closed end. The set of these points is:

$$\begin{aligned} \mathcal{F} &= \{f_i \mid f_i = f_{min} + i\Delta f\} \subset S_{\mathcal{F}} \\ &= \{f_0, f_1, \ldots, f_{N_f - 1}\} \end{aligned} \tag{15}$$

$\mathcal{F}$ is a discretization of $S_{\mathcal{F}}$ and may be thought of as a set of audible frequencies.

The sound pressure space is constructed similarly to yield:

$$\begin{aligned} &a. \quad \mathcal{P} = \{p_1, p_2, \ldots, p_{N_P}\} \subset S_{\mathcal{P}} \text{ (set of audible pressures)} \\ &b. \quad \mathcal{H}_{\mathcal{P}} = \{h_p \mid h_p = [p, p + \Delta p) \mid p \in \mathcal{P}\} \text{ (set of half open intervals)} \\ &c. \quad \tau_{\mathcal{P}} = \{\bigcup H_p \mid H_p \subseteq \mathcal{H}_{\mathcal{P}}\} \text{ (topology of } S_{\mathcal{P}}) \end{aligned} \tag{16}$$

The basis for a topology in $\mathcal{A} = S_{\mathcal{F}} \times S_{\mathcal{P}}$ is:

$$\mathcal{B}_{\mathcal{A}} = \{U_f \times U_p \mid U_f \subset \mathcal{H}_{\mathcal{F}}, U_p \subset \mathcal{H}_p\} \tag{17}$$

The topology for $\mathcal{A}$ is:

$$\tau_{\mathcal{A}} = \{\bigcup A \mid A \subseteq \mathcal{B}_{\mathcal{A}}\} \tag{18}$$

If only the sets of audible frequencies and pressures are considered, then the discretized acoustic space is:

$$\mathcal{A} = \mathcal{F} \times \mathcal{P} \tag{19}$$

with the discrete topology.

Neural Space

The neural space $S_{\mathcal{X}}$ is constructed in a similar fashion as $\mathcal{F}$ and $\mathcal{P}$, though the topology is slightly different. The idea is to partition $S_{\mathcal{X}}$ into subintervals that represent neurons and then to combine the subintervals contiguously to form synaptic intervals.

The neural space $S_{\mathcal{X}} \subset \mathbb{R}^+$ is a half-open interval representing the one dimensional tonotopic axis: $S_{\mathcal{X}} = [x_{min}, x_{max})$. $S_{\mathcal{X}}$ is partitioned into N_{cell} half-open intervals, each of width Δx and expressed as $[x_\alpha, x_\beta), x_\beta > x_\alpha$ or $[x_\alpha, x_\alpha + \Delta x)$. Each interval represents the length (Δx) of a single cell on the tonotopic axis. The set of intervals is expressed as:

$$\begin{aligned} \mathcal{H}_{x,1} &= \{h_{x_i,1} = [x_i, x_i + \Delta x)) \mid x_i \in S_{\mathcal{X}}, x_i \leq |S_{\mathcal{X}}| - \Delta x\} \\ &= \{h_{x,1} = [x_{min} + i\Delta x, x_{min} + (i+1)\Delta x) \mid i \in \mathbb{N}_0, i < N_{cell}\} \end{aligned} \tag{20}$$

The set $\mathcal{H}_{x,1}$ is a partition, which effectively discretizes $\mathcal{X}$ (see section above for a similar treatment). Each interval is uniquely identified by the point at the closed end (x_i in eq. 20). The set $\mathcal{X}$ containing these points is:

$$\begin{aligned} \mathcal{X} &= \{x_i \mid x_i = x_{min} + i\Delta x \mid x_i \in S_{\mathcal{X}}, 0 < i < N_{cell}\} \\ &= \{x_0, x_1, \ldots, x_{N_{cell}-1}\} \end{aligned} \tag{21}$$

A synaptic interval is also a half-open interval with length λ expressed as:

$$h_{x,\lambda} = [x, x + \lambda),\ x \in \mathcal{X}, \lambda \in S_\Lambda$$

where $S_\Lambda = [\lambda_{\min}, \lambda_{\max})$, $\lambda_{min} > 0, \lambda_{max} < |S_{\mathcal{X}}|$ is the range of values that the length can take. The length of the synaptic interval is defined to be a contiguous set of cells so that $h_{x,\lambda}$ is an integral multiple of cell length Δx. Letting $n_\lambda \in \mathbb{N}^+$ be the number of cells in the interval, the intervals may be re-expressed as:

$$h_{x,\lambda} = [x, x + \lambda),\ x \in \mathcal{X}, \lambda = n_\lambda \Delta x, n_\lambda \leq n_{\lambda,max} \leq N_{cells} \tag{22}$$

where $n_{\lambda,max}$ is the maximum number of cells in the interval. The set containing all possible interval lengths is :

$$\begin{aligned} \Lambda &= \{\lambda_{n_\lambda} \mid \lambda_{n_\lambda} = n\Delta x, n_\lambda \leq n_{\lambda,max} \leq N_{cell}\} \subset S_\Lambda \\ &= \{\lambda_1, \lambda_2, \ldots, \lambda_{max}\} \end{aligned} \tag{23}$$

As shown in the next section, sound pressure will be encoded as the length of the intervals. In order to ensure a full representation of sound pressure, a 'buffer' of $N_{cell} - n_{\max}$ cells is needed. Without the buffer, the maximum value of last interval is 1 cell. The set of identifying points for synaptic intervals is then:

$$\mathcal{X}_\lambda = \{x_1, x_2, \ldots, x_{N_\lambda}\} \subset \mathcal{X}; N_\lambda = N_{cell} - n_{max} \tag{24}$$

The set of synaptic intervals is expressed as:

$$\mathcal{H}_{x,\lambda} = \{h_{x,\lambda} = [x, x+\lambda) \mid x \in \mathcal{X}, \lambda \in \Lambda\} \tag{25}$$

The topology of $S_\mathcal{X}$ generated by the elements of $\mathcal{H}_{x,\lambda}$ is:

$$\tau_\mathcal{X} = \{\bigcup H_s \mid H_s \subseteq \mathcal{H}_{x,\lambda}\} \tag{26}$$

Mapping from acoustic space to neural space

The aim is to construct a mapping between the acoustic and neural spaces in such a way that allows for both encoding and decoding sounds in neural space.

Note that a pure tone $a_{f,p}$ corresponds to the ordered pair $(f, p) \in S_\mathcal{F} \times S_\mathcal{P}$ and an interval $h_{x,\lambda} = [x, x+\lambda)$ corresponds to the ordered pair $(x, \lambda) \in S_\mathcal{X} \times S_\Lambda$. The mapping (ψ) from acoustic to neural space is obtained by first defining mappings from frequency space $(S_\mathcal{F})$ to neural space $(S_\mathcal{X})$ and from pressure space $(S_\mathcal{P})$ to interval length space (S_Λ):

$$\begin{aligned} &\psi_f : S_\mathcal{F} \to \mathcal{X}, \psi_f(f) = x; \\ &\psi_p : S_\mathcal{P} \to S_\Lambda, \psi_p(p) = \lambda; \\ &\psi : S_\mathcal{F} \times S_\mathcal{P} \to S_\mathcal{X} \times S_\Lambda; \psi(f, p) = (\psi_f(f), \psi_p(p)) = (x, \lambda) \end{aligned} \tag{27}$$

By construction, the mappings are homeomorphisms.

After partitioning, the spaces are effectively discretized into $\mathcal{F} \subset S_\mathcal{F}, \mathcal{P} \subset S_\mathcal{P}, \mathcal{X}_\lambda \subset S_\mathcal{X}, \Lambda \subset S_\Lambda$. These are the functionally and biological relevant sets as they contain the audible frequencies and pressures that can be mapped into the compartmentalized neural space. Therefore, the mapping can be restricted to these sets:

$$\begin{aligned} &\psi_f\restriction_\mathcal{F} : \mathcal{F} \to \mathcal{X}_\lambda, \psi_f\restriction_\mathcal{F}(f) = x; \\ &\psi_p\restriction_\mathcal{P} : \mathcal{P} \to \lambda, \psi_p\restriction_\mathcal{P}(p) = \lambda; \\ &\psi\restriction_{\mathcal{F},\mathcal{P}} : \mathcal{F} \times \mathcal{P} \to \mathcal{X} \times \Lambda; \psi\restriction_{\mathcal{F},\mathcal{P}}(f, p) \\ &= (\psi_f\restriction_\mathcal{F}(f), \psi_p\restriction_\mathcal{P}(p)) = (x, \lambda) \end{aligned} \tag{28}$$

The maps are bijective if $|\mathcal{F}| = |\mathcal{X}_\lambda|$ and $|\mathcal{P}| = |\Lambda|$ and continuous because the restricted spaces have the discrete topology.

Algebraic operations

In the following, addition and multiplication operations for combining elements in acoustic and neural spaces are defined.

Operations in acoustic space

Complex sounds are composed of multiple pure tones of varying frequencies and intensities. The analyses will be limited to sets of audible frequencies ($\mathcal{F}$) and pressures ($\mathcal{P}$). Pure tones are combined with an addition ("+") operation defined as the 'union'.

$$+ : \mathcal{A} \times \mathcal{A} \to \mathcal{A}; a_{f_\alpha,p_\alpha} + a_{f_\beta,p_\beta} \stackrel{\text{def}}{=} a_{f_\alpha,p_\alpha} \cup a_{f_\beta,p_\beta} \tag{29}$$

One property that is potentially problematic is that the addition operation can produce a sound with the same frequency but different pressures, which is physically impossible (e.g. $a_{f_\alpha,p_\gamma} \cup a_{f_\alpha,p_\delta} = \{a_{f_\alpha,p_\gamma}, a_{f_\alpha,p_\delta}\}$). This may actually be a desirable property because the sound information may propagate through different channels in the auditory pathway before converging to a neural space (e.g. binaural stimuli). Nevertheless, assigning multiple pressure values to a single frequency may be avoided as follows. For $a_{f_\alpha,p_\alpha}, a_{f_\beta,p_\beta} \in \mathcal{A}$,

$$\begin{aligned} &a_{f_\alpha,p_\alpha} + a_{f_\beta,p_\beta} = \\ &\quad \begin{cases} \{a_{f_\alpha,p_\alpha}, a_{f_\beta,p_\beta}\}, & f_\alpha \neq f_\beta \\ a_{f,p_\gamma},\ p_\gamma = \max(p_\alpha, p_\beta), & f_\alpha = f_\beta \end{cases} \end{aligned} \tag{30}$$

Operations in Neural Space

In neural space, addition ("+") is also defined as the union. For $h_{x_\alpha\lambda_\alpha}, h_{x_\beta\lambda_\beta} \in (S_\mathcal{X}, \tau_\mathcal{X})$

$$\begin{aligned} &+ : (S_\mathcal{X}, \tau_\mathcal{X}) \times (S_\mathcal{X}, \tau_\mathcal{X}) \to (S_\mathcal{X}, \tau_\mathcal{X}); \\ &h_{x_\alpha\lambda_\alpha} + h_{x_\beta\lambda_\beta} \stackrel{\text{def}}{=} h_{x_\alpha\lambda_\alpha} \cup h_{x_\beta\lambda_\beta} \end{aligned} \tag{31}$$

Generally, for any two synaptic intervals $(h_{x\lambda_\alpha}, h_{x\lambda_\beta})$, the addition operation yields two possibilities:

$$\begin{aligned} &h_{x_\alpha\lambda_\alpha} + h_{x_\beta\lambda_\beta} = \\ &\quad \begin{cases} h_{x\lambda}, x = \min(x_\alpha, x_\beta), \lambda = |h_{x\lambda_\alpha} \cup h_{x\lambda_\beta}|, & h_{x\lambda_\alpha} \cap h_{x\lambda_\beta} \neq \emptyset \\ \{h_{x_\alpha\lambda_\alpha}, h_{x_\beta\lambda_\beta}\}, & h_{x\lambda_\alpha} \cap h_{x\lambda_\beta} = \emptyset \end{cases} \end{aligned} \tag{32}$$

For more than 2 synaptic intervals, the total length λ is given by the Inclusion-Exclusion principle.

The algebraic structure on $(S_\mathcal{X}, \tau_\mathcal{X})$ with the addition operation is a monoid since it inherits the algebraic properties of the union operation. In particular, addition is closed because the result is either a longer, half-open interval or two disjoint half-open intervals, either of which is an element of $\tau_\mathcal{X}$. Addition is commutative, associative, has the empty set as the identity element, and does not have an inverse.

Multiplication "$\cdot$" of synaptic intervals is defined as the set minus operation ($\setminus$). Given two intervals $h_{x_\alpha,\lambda_\alpha}, h_{x_\beta,\lambda_\beta} \in (S_\mathcal{X}, \tau_\mathcal{X})$ where $h_{x_\alpha,\lambda_\alpha}$ is the multiplier and $h_{x_\beta,\lambda_\beta}$ is the multiplicand,

$$\begin{aligned} &\bullet : (S_\mathcal{X}, \tau_\mathcal{X}) \times (S_\mathcal{X}, \tau_\mathcal{X}) \to (S_\mathcal{X}, \tau_\mathcal{X}); \\ &h_{x_\alpha,\lambda_\alpha} \cdot h_{x_\beta,\lambda_\beta} \stackrel{\text{def}}{=} h_{x_\beta,\lambda_\beta} \setminus h_{x_\alpha,\lambda_\alpha} \end{aligned} \tag{33}$$

Letting $\hat{\lambda} = |h_{x_\beta,\lambda_\beta} \setminus h_{x_\alpha,\lambda_\alpha}|$, the possible results of multiplication are:

$$
\begin{aligned}
&h_{x_\alpha,\lambda_\alpha} \cdot h_{x_\beta,\lambda_\beta} = \\
&\quad \begin{cases}
1.\, h_{x_\beta,\lambda_\beta}, & h_{x_\alpha,\lambda_\alpha} \cap h_{x_\beta,\lambda_\beta} = \emptyset \\
2.\, [x_\beta, x_\beta + \hat{\lambda}), & h_{x_\alpha,\lambda_\alpha} \cap h_{x_\beta,\lambda_\beta} \neq \emptyset, x_\beta < x_\alpha, h_{x_\alpha,\lambda_\alpha} \not\subset h_{x_\beta,\lambda_\beta} \\
3.\, [x_\delta, x_\delta + \hat{\lambda}), & h_{x_\alpha,\lambda_\alpha} \cap h_{x_\beta,\lambda_\beta} \neq \emptyset, x_\beta \geq x_\alpha, h_{x_\beta,\lambda_\beta} \not\subset h_{x_\alpha,\lambda_\alpha} \\
\qquad x_\delta = x_\beta + (\lambda_\beta - \hat{\lambda}) & \\
4.\, \emptyset, & h_{x_\beta,\lambda_\beta} \subset h_{x_\alpha,\lambda_\alpha} \\
5.\, \{[x_\beta, x_\alpha), [x_\alpha + \lambda_\alpha, x_\beta + \lambda_\beta)\}, & h_{x_\alpha,\lambda_\alpha} \subset h_{x_\beta,\lambda_\beta}
\end{cases}
\end{aligned}
\tag{34}
$$

The algebraic structure on $(S_\mathcal{X}, \tau_X)$ with the multiplication operation is a magma, with properties inherited from the set minus operation. Multiplication is closed because the set minus operation yields an interval that is either the empty set or a half-open interval(s) with a minimum length(s) of Δx and maximum length of λ_{max}. In either case, the resulting interval is in $(S_\mathcal{X}, \tau_\mathcal{X})$. While the $\emptyset$ is a left identity element, there is no unique inverse element since the result is the $\emptyset$ whenever the length of multiplier is greater than or equal to that of the multiplicand. It is also neither commutative nor associative.

Proposition 0.0.1. The *multiplication* operation is left but not right distributive over addition.

Proof. **Left distributive**: Let $h_{x_\alpha,\lambda_\alpha}, h_{x_\beta,\lambda_\beta}, h_{x_\gamma,\lambda_\gamma} \in (S_\mathcal{X}, \tau_\mathcal{X})$

$$
\begin{aligned}
&= h_{x_\gamma,\lambda_\gamma} \cdot (h_{x_\alpha,\lambda_\alpha} + h_{x_\beta,\lambda_\beta}) \\
&= (h_{x_\alpha,\lambda_\alpha} \cup h_{x_\beta,\lambda_\beta}) \setminus h_{x_\gamma,\lambda_\gamma} \\
&= h^c_{x_\gamma,\lambda_\gamma} \cap (h_{x_\alpha,\lambda_\alpha} \cup h_{x_\beta,\lambda_\beta}), \text{ 'c' is complement} \\
&= (h^c_{x_\gamma,\lambda_\gamma} \cap h_{x_\alpha,\lambda_\alpha}) \cup (h^c_{x_\gamma,\lambda_\gamma} \cap h_{x_\beta,\lambda_\beta}) \\
&= h_{x_\alpha,\lambda_\alpha} \setminus h_{x_\gamma,\lambda_\gamma} \cup h_{x_\beta,\lambda_\beta} \setminus h_{x_\gamma,\lambda_\gamma} \\
&= h_{x_\gamma,\lambda_\gamma} \cdot h_{x_\alpha,\lambda_\alpha} + h_{x_\gamma,\lambda_\gamma} \cdot h_{x_\beta,\lambda_\beta}
\end{aligned}
$$

Not Right distributive:

$$
\begin{aligned}
&(h_{x_\alpha,\lambda_\alpha} + h_{x_\beta,\lambda_\beta}) \cdot h_{x_\gamma,\lambda_\gamma} \\
&= h_{x_\gamma,\lambda_\gamma} \setminus (h_{x_\alpha,\lambda_\alpha} \cup h_{x_\beta,\lambda_\beta}) \\
&= h_{x_\gamma,\lambda_\gamma} \cap (h_{x_\alpha,\lambda_\alpha} \cup h_{x_\beta,\lambda_\beta})^c \\
&= h_{x_\gamma,\lambda_\gamma} \cap (h^c_{x_\alpha,\lambda_\alpha} \cap h^c_{x_\beta,\lambda_\beta}), \text{from de Morgan's law} \\
&\neq h_{x_\alpha,\lambda_\alpha} \cdot h_{x_\gamma,\lambda_\gamma} + h_{x_\beta,\lambda_\beta} \cdot h_{x_\gamma,\lambda_\gamma}
\end{aligned}
$$

□

While not Right distributive, a notable property is that the effect of two multipliers acting on a single multiplicand is that the operation can be performed sequentially:

$$
\begin{aligned}
&h_{x_\gamma,\lambda_\gamma} \cap (h^c_{x_\alpha,\lambda_\alpha} \cap h^c_{x_\beta,\lambda_\beta}), \text{(from Proposition 0.0.1)} \\
&= (h_{x_\gamma,\lambda_\gamma} \cap h^c_{x_\alpha,\lambda_\alpha}) \cap h^c_{x_\beta,\lambda_\beta} = (h_{x_\gamma,\lambda_\gamma} \cap h^c_{x_\beta,\lambda_\beta}) \cap h^c_{x_\alpha,\lambda_\alpha} \\
&= (h_{x_\gamma,\lambda_\gamma} \setminus h_{x_\alpha,\lambda_\alpha}) \setminus h_{x_\beta,\lambda_\beta} = (h_{x_\gamma,\lambda_\gamma} \setminus h_{x_\beta,\lambda_\beta}) \setminus h_{x_\alpha,\lambda_\alpha} \\
&= h_{x_\beta,\lambda_\beta} \cdot (h_{x_\alpha,\lambda_\alpha} \cdot h_{x_\gamma,\lambda_\gamma}) = h_{x_\alpha,\lambda_\alpha} \cdot (h_{x_\beta,\lambda_\beta} \cdot h_{x_\gamma,\lambda_\gamma})
\end{aligned}
$$

Place code with columnar organization and population rate code

In the mathematical model, the 'functional' unit is an interval that can vary in size, depending on the sound intensity. The indistinct borders are consistent with topographical organization of afferents [19]. An alternative organization is with classical columns [17]. The definition of a column has evolved [50] but for illustrative purposes, columns are defined here as having distinct borders; the enclosed neurons have identical receptive fields and hence function as a single unit. In this scheme, the location of the active column encodes frequency. Because the column dimension is fixed, sound pressure will be encoded as the average number of neurons that become active during the stimulus.

The number ($|\mathcal{F}|$) of frequencies that can be encoded in neural space depends on the column dimension. The neural space is partitioned into N_{cell}, non-overlapping half-open intervals to represent neurons (see above). The columns are also non-overlapping half open intervals, consisting of a contiguous set of n_{cell} neurons. Thus, the number of columns N_{col} that can fit into the neural space is $N_{col} = N_{cell}/n_{col}$. To construct a bijective mapping between acoustic and neural space, the number of frequency elements must be equal to that in neural space, that is: $|\mathcal{F}| = N_{cell}/n_{col}$. Therefore, $|\mathcal{F}|$ is maximal when $n_{col} = 1$ and decreases hyperbolically thereafter.

The number of cells (n_{on}) in a column that becomes active during a stimulus is taken to be proportional to the stimulus intensity. Therefore, the number of levels that can be represented is limited by the number of cells in each column. Hence, for bijective mapping from pressure ($\mathcal{P}$) to cells in the columns, $|\mathcal{P}| = n_{col}$, which is inverse of the condition for maximizing $|\mathcal{F}|$. This means that the increasing the number of frequency levels comes at the expense of the number of pressure levels and vice-versa.

The one potential advantage of a columnar organization/population rate code is that sounds with multiple tonal components can be more accurately encoded. Unlike with overlapping intervals, the representation of frequency components in neural space remain separated because the columns are disjoint. Thus, there are no ambiguities when the sound is composed of tones with similar frequencies.

Experimental evidence

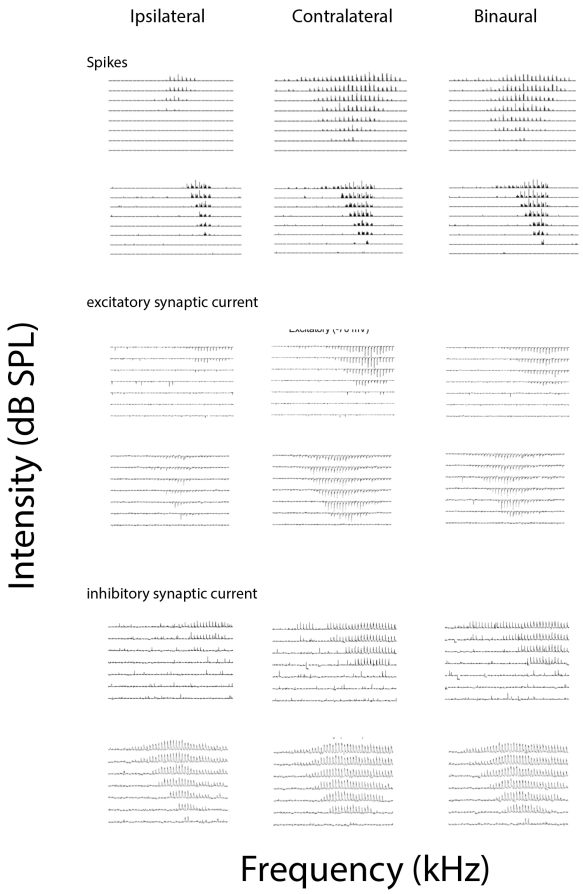

Experimental evidence for Addition operation Data from reference [26]. Extracellular (top) and whole-cell voltage clamp (middle, bottom) recording from the central nucleus of the Inferior colliculus, which receives binaural inputs. The frequency response areas (FRA) were constructed by presenting pure tones of varying frequencies (abscissas) and intensities (ordinates) and documenting the responses. Tones were delivered to ipsilaterally (left column), contralaterally (middle), and binaurally (right). As mentioned in the main text, the FRAs can be taken as an indicator of the spatial extent of synaptic field and activated area. The model predicts that because the contralateral response is greater than the ipsilateral response, the response evoked with binaural stimulation should equal that of contralateral stimulation. In all cases, the binaural FRAs was nearly identical to the contralateral FRAs. *Permission pending.*

References

[1] William M Siebert. "Frequency discrimination in the auditory system: Place or periodicity mechanisms?" In: *Proceedings of the IEEE* 58.5 (1970), pp. 723–730.

[2] Georg Von Bekesy and Ernest Glen Wever. *Experiments in hearing*. Vol. 8. McGraw-Hill New York, 1960.

[3] Jozef J Zwislocki and My Nguyen. "Place code for pitch: A necessary revision". In: *Acta oto-laryngologica* 119.2 (1999), pp. 140–145.

[4] Troy A Hackett et al. "Linking topography to tonotopy in the mouse auditory thalamocortical circuit". In: *Journal of Neuroscience* 31.8 (2011), pp. 2983–2995.

[5] Brian CJ Moore and Stephan MA Ernst. "Frequency difference limens at high frequencies: evidence for a transition from a temporal to a place code". In: *The Journal of the Acoustical Society of America* 132.3 (2012), pp. 1542–1547.

[6] Robert P Carlyon et al. "Pitch comparisons between electrical stimulation of a cochlear implant and acoustic stimuli presented to a normal-hearing contralateral ear". In: *Journal of the Association for Research in Otolaryngology* 11.4 (2010), pp. 625–640.

[7] Bertrand Delgutte. "Physiological models for basic auditory percepts". In: *Auditory computation*. Springer, 1996, pp. 157–220.

[8] JM Doughty and WR Garner. "Pitch characteristics of short tones. II. Pitch as a function of tonal duration." In: *Journal of Experimental Psychology* 38.4 (1948), p. 478.

[9] Brian CJ Moore. "Frequency difference limens for short-duration tones". In: *The Journal of the Acoustical Society of America* 54.3 (1973), pp. 610–619.

[10] Christophe Micheyl, Li Xiao, and Andrew J Oxenham. "Characterizing the dependence of pure-tone frequency difference limens on frequency, duration, and level". In: *Hearing Research* 292.1-2 (2012), pp. 1–13.

[11] Christophe Micheyl, Paul R Schrater, and Andrew J Oxenham. "Auditory frequency and intensity discrimination explained using a cortical population rate code". In: *PLoS computational biology* 9.11 (2013), e1003336.

[12] Brenda J Hefti and Philip H Smith. "Anatomy, Physiology, and Synaptic Responses of Rat Layer V Auditory Cortical Cells and Effects of Intracellular GABAABlockade". In: *Journal of Neurophysiology* 83.5 (2000), pp. 2626–2638.

[13] Anne-Marie M Oswald and Alex D Reyes. "Maturation of intrinsic and synaptic properties of layer 2/3 pyramidal neurons in mouse auditory cortex". In: *Journal of neurophysiology* 99.6 (2008), pp. 2998–3008.

[14] AD Reyes, EW Rubel, and WJ Spain. "Membrane properties underlying the firing of neurons in the avian cochlear nucleus". In: *Journal of Neuroscience* 14.9 (1994), pp. 5352–5364.

[15] Xiaoqin Wang et al. "Neural coding of temporal information in auditory thalamus and cortex". In: *Neuroscience* 154.1 (2008), pp. 294–303.

[16] Mounya Elhilali et al. "Dynamics of precise spike timing in primary auditory cortex". In: *Journal of Neuroscience* 24.5 (2004), pp. 1159–1172.

[17] Vernon B Mountcastle. "Modality and topographic properties of single neurons of cat's somatic sensory cortex". In: *Journal of neurophysiology* 20.4 (1957), pp. 408–434.

[18] David H Hubel and Torsten N Wiesel. "Receptive fields, binocular interaction and functional architecture in the cat's visual cortex". In: *The Journal of physiology* 160.1 (1962), pp. 106–154.

[19] Arnold L Towe. "Notes on the Hypothesis of Columnar Organization in Somatosensory Cerebral Cortex; pp. 32–47". In: *Brain, Behavior and Evolution* 11.1 (1975), pp. 32–47.

[20] Christoph E Schreiner. "Spatial distribution of responses to simple and complex sounds in the primary auditory cortex". In: *Audiology and Neurotology* 3.2-3 (1998), pp. 104–122.

[21] Tianying Ren, Wenxuan He, and David Kemp. "Reticular lamina and basilar membrane vibrations in living mouse cochleae". In: *Proceedings of the National Academy of Sciences* 113.35 (2016), pp. 9910–9915.

[22] Monita Chatterjee and Jozef J Zwislocki. "Cochlear mechanisms of frequency and intensity coding. I. The place code for pitch". In: *Hearing research* 111.1-2 (1997), pp. 65–75.

[23] William M Siebert et al. "Stimulus transformations in the peripheral auditory system". In: *Recognizing patterns* 104.133 (1968), pp. 602–615.

[24] Robert B Levy and Alex D Reyes. "Coexistence of lateral and co-tuned inhibitory configurations in cortical networks". In: *PLoS computational biology* 7.10 (2011), e1002161.

[25] Robert B Levy and Alex D Reyes. "Spatial profile of excitatory and inhibitory synaptic connectivity in mouse primary auditory cortex". In: *Journal of Neuroscience* 32.16 (2012), pp. 5609–5619.

[26] Xiaorui R Xiong et al. "Interaural level difference-dependent gain control and synaptic scaling underlying binaural computation". In: *Neuron* 79.4 (2013), pp. 738–753.

[27] Michael Epstein and Mary Florentine. "Binaural loudness summation for speech presented via earphones and loudspeaker with and without visual cues". In: *The Journal of the Acoustical Socient of America* 131 (2012), pp. 3981–3988.

[28] Alex Reyes et al. "Target-cell-specific facilitation and depression in neocortical circuits". In: *Nature neuroscience* 1.4 (1998), pp. 279–285.

[29] WR Thurlow and S Bernstein. "Simultaneous Two-Tone Pitch Discrimination". In: *The Journal of the Acoustical Society of America* 29.4 (1957), pp. 515–519.

[30] Willard R Thurlow and Irving L Rawlings. "Discrimination of number of simultaneously sounding tones". In: *The Journal of the Acoustical Society of America* 31.10 (1959), pp. 1332–1336.

[31] Christophe NJ Stoelinga and Robert A Lutfi. "Discrimination of the spectral density of multitone complexes". In: *The Journal of the Acoustical Society of America* 130.5 (2011), pp. 2882–2890.

[32] Bertram Scharf. "Complex sounds and critical bands." In: *Psychological Bulletin* 58.3 (1961), p. 205.

[33] Eberhard Zwicker, Georg Flottorp, and Stanley Smith Stevens. "Critical band width in loudness summation". In: *The Journal of the Acoustical Society of America* 29.5 (1957), pp. 548–557.

[34] Imme Stiebler and Gunter Ehret. "Inferior colliculus of the house mouse. I. A quantitative study of tonotopic organization, frequency representation, and tone-threshold distribution". In: *Journal of Comparative Neurology* 238.1 (1985), pp. 65–76.

[35] Feng Luo et al. "Three-dimensional tonotopic organization of the C57 mouse cochlear nucleus". In: *Hearing research* 257.1-2 (2009), pp. 75–82.

[36] I Stiebler et al. "The auditory cortex of the house mouse: left-right differences, tonotopic organization and quantitative analysis of frequency representation". In: *Journal of Comparative Physiology A* 181.6 (1997), pp. 559–571.

[37] Wei Guo et al. "Robustness of cortical topography across fields, laminae, anesthetic states, and neurophysiological signal types". In: *Journal of Neuroscience* 32.27 (2012), pp. 9159–9172.

[38] John B Issa et al. "Multiscale optical Ca2+ imaging of tonal organization in mouse auditory cortex". In: *Neuron* 83.4 (2014), pp. 944–959.

[39] Daniel E Winkowski and Patrick O Kanold. "Laminar transformation of frequency organization in auditory cortex". In: *Journal of Neuroscience* 33.4 (2013), pp. 1498–1508.

[40] Gideon Rothschild, Israel Nelken, and Adi Mizrahi. "Functional organization and population dynamics in the mouse primary auditory cortex". In: *Nature neuroscience* 13.3 (2010), p. 353.

[41] Sharba Bandyopadhyay, Shihab A Shamma, and Patrick O Kanold. "Dichotomy of functional organization in the mouse auditory cortex". In: *Nature neuroscience* 13.3 (2010), p. 361.

[42] JJ Zwislocki. "What is the cochlear place code for pitch?" In: *Acta oto-laryngologica* 111.2 (1991), pp. 256–262.

[43] ML Sutter et al. "Organization of inhibitory frequency receptive fields in cat primary auditory cortex". In: *Journal of Neurophysiology* 82.5 (1999), pp. 2358–2371.

[44] Rishidev Chaudhuri and Ila Fiete. "Computational principles of memory". In: *Nature neuroscience* 19.3 (2016), p. 394.

[45] Jeremie Barral, Xiao-Jing Wang, and Alex D Reyes. "Propagation of temporal and rate signals in cultured multilayer networks". In: *Nature communications* 10.1 (2019), pp. 1–14.

[46] Jian Wang, Donald Caspary, and Richard J Salvi. "GABA-A antagonist causes dramatic expansion of tuning in primary auditory cortex". In: *Neuroreport* 11.5 (2000), pp. 1137–1140.

[47] Fiona EN LeBeau, Manuel S Malmierca, and Adrian Rees. "Iontophoresis in vivo demonstrates a key role for GABAA and glycinergic inhibition in shaping frequency response areas in the inferior colliculus of guinea pig". In: *Journal of Neuroscience* 21.18 (2001), pp. 7303–7312.

[48] Carina Curto et al. "Combinatorial neural codes from a mathematical coding theory perspective". In: *Neural computation* 25.7 (2013), pp. 1891–1925.

[49] Leslie C Osborne et al. "The neural basis for combinatorial coding in a cortical population response". In: *Journal of Neuroscience* 28.50 (2008), pp. 13522–13531.

[50] Jonathan C Horton and Daniel L Adams. "The cortical column: a structure without a function". In: *Philosophical Transactions of the Royal Society B: Biological Sciences* 360.1456 (2005), pp. 837–862.